

Regulation of AMP-activated protein kinase by a pseudosubstrate sequence on the γ subunit

John W Scott¹, Fiona A Ross, JK David Liu and D Grahame Hardie*

Division of Molecular Physiology, College of Life Sciences, University of Dundee, Sir James Black Centre, Dundee, UK

The AMP-activated protein kinase (AMPK) system monitors cellular energy status by sensing AMP and ATP, and is a key regulator of energy balance at the cellular and whole-body levels. AMPK exists as heterotrimeric $\alpha\beta\gamma$ complexes, and the γ subunits contain two tandem domains that bind the regulatory nucleotides. There is a sequence in the first of these domains that is conserved in γ subunit homologues in all eukaryotes, and which resembles the sequence around sites phosphorylated on target proteins of AMPK, except that it has a non-phosphorylatable residue in place of serine. We propose that in the absence of AMP this pseudosubstrate sequence binds to the active site groove on the α subunit, preventing phosphorylation by the upstream kinase, LKB1, and access to downstream targets. Binding of AMP causes a conformational change that prevents this interaction and relieves the inhibition. We present several lines of evidence supporting this hypothesis.

The EMBO Journal (2007) 26, 806–815. doi:10.1038/sj.emboj.7601542; Published online 25 January 2007

Subject Categories: signal transduction; structural biology

Keywords: AMP; AMP-activated protein kinase; energy balance; LKB1; pseudosubstrate

Introduction

The AMP-activated protein kinase (AMPK) is the downstream component of a highly conserved protein kinase cascade that plays a key role in metabolic regulation, particularly in response to stresses that cause ATP depletion (Hardie *et al.*, 2003; Hardie, 2004; Hardie and Sakamoto, 2006). The AMPK cascade monitors cellular energy charge, being activated by a rising AMP:ATP ratio caused by metabolic stresses such as glucose deprivation, hypoxia, ischaemia, and (in muscle) exercise or contraction. In the short term, activation of AMPK promotes conservation of ATP by directly phosphorylating metabolic enzymes, resulting in the inhibition of ATP-consuming pathways and activation of ATP-generating catabolic pathways. Activation of AMPK also results in chronic metabolic adaptations, including decreased expression of

lipogenic and gluconeogenic enzymes, and increased mitochondrial biogenesis. As well as responding to metabolic stress, AMPK is regulated by adipokines such as leptin (Minokoshi *et al.*, 2002) and adiponectin (Tomas *et al.*, 2002; Yamauchi *et al.*, 2002), and by various drugs. The latter include 5-aminoimidazole-4-carboxamide riboside (Corton *et al.*, 1995), which in animal models reverses many of the abnormalities of the metabolic syndrome (Hardie, 2004; Hardie and Sakamoto, 2006), and the widely used anti diabetic drugs metformin (Zhou *et al.*, 2001) and thiazolidinediones (Fryer *et al.*, 2002; Saha *et al.*, 2004). Recent studies suggest that AMPK activation accounts for the therapeutic effects of metformin (Shaw *et al.*, 2005), a drug prescribed to 120 million people worldwide. Thus, AMPK has become an attractive target for development of new drugs aimed at treatment of type II diabetes, obesity and the metabolic syndrome. One way to develop new drugs would be to determine the mechanism by which AMPK is regulated by its natural activator 5'-AMP.

AMPK is a heterotrimer composed of a catalytic subunit (α) and two regulatory subunits (β and γ) (Hardie *et al.*, 2003). Each subunit is encoded by two or three genes that can also be subject to alternative splicing, leading to a diverse array of $\alpha\beta\gamma$ complexes that display differences in regulation and subcellular localization (Salt *et al.*, 1998; Cheung *et al.*, 2000). Regulation of mammalian AMPK is complex, involving both direct allosteric activation and reversible phosphorylation. The enzyme is activated by phosphorylation of Thr-172 within the activation loop of the kinase domain by protein complexes containing LKB1, a serine/threonine protein kinase that is a tumour suppressor, and is mutated in Peutz-Jeghers syndrome, an inherited predisposition to cancer (Hawley *et al.*, 2003; Woods *et al.*, 2003; Shaw *et al.*, 2004). In some tissues, Ca^{2+} /calmodulin-dependent protein kinase kinases, especially CaMKK β , are alternate upstream kinases that activate AMPK in a Ca^{2+} -activated manner (Hawley *et al.*, 2005; Hurley *et al.*, 2005; Woods *et al.*, 2005). Binding of AMP to AMPK causes activation by three distinct mechanisms, all of which are antagonized by high concentrations of ATP (Hardie *et al.*, 1999): (i) by direct allosteric activation; (ii) by inducing a conformational change that makes it a better substrate for LKB1; (iii) by inducing a conformational change that makes it a worse substrate for inactivating protein phosphatases. This complex mechanism allows the AMPK system to respond to small changes in cellular energy status in a highly sensitive manner (Hardie *et al.*, 1999).

All three γ subunit isoforms of AMPK ($\gamma 1$, $\gamma 2$, $\gamma 3$) contain two tandem Bateman domains (Kemp, 2004), each of which is itself a tandem repeat of a CBS motif (Bateman, 1997). Recently, we reported that Bateman domains form binding sites for adenosine-containing ligands, with the domains in the γ subunits of AMPK forming two-binding sites for the activating nucleotide AMP to which ATP also binds in a mutually exclusive manner (Scott *et al.*, 2004). However, an unresolved problem in the AMPK field has been the

*Corresponding author. Division of Molecular Physiology, College of Life Sciences, University of Dundee, Sir James Black Centre, Dow Street, Dundee DD1 5EH, UK. Tel.: +44 1382 384253;

Fax: +44 1382 385507; E-mail: d.g.hardie@dundee.ac.uk

¹Present address: St Vincents Institute of Medical Research, 41 Victoria Parade, Fitzroy, Victoria 3065, Australia

Received: 26 June 2006; accepted: 14 December 2006; published online: 25 January 2007

mechanism by which binding of AMP activates the kinase and promotes its phosphorylation by the upstream kinase (Hawley *et al*, 1995, 2003). Other ligand-activated protein kinases contain pseudosubstrate sequences that resemble the sequences at target phosphorylation sites (Kemp *et al*, 1994). These act as auto-inhibitory sequences that bind to the protein substrate-binding groove in the kinase domain and inhibit the kinase in the absence of the activating ligand, as observed in the crystal structure of calmodulin-dependent protein kinase I (Goldberg *et al*, 1996). These sequences are usually located adjacent to, or overlapping with, the ligand-binding domain, and binding of the activating ligand is thought to cause a conformational change that prevents the auto-inhibitory interaction (Kemp *et al*, 1994).

We report that the second CBS motif of the γ subunits of AMPK contains a pseudosubstrate sequence that resembles sites phosphorylated by AMPK on target proteins, but which lacks a phosphorylatable amino acid. We provide evidence that this sequence inhibits the kinase domain on the α subunit in the absence of AMP, and that the binding of AMP prevents this auto-inhibitory interaction.

Results

Identification of a pseudosubstrate sequence on the γ subunits of AMPK

Using variant synthetic peptides and site-directed mutagenesis of a protein substrate (Weekes *et al*, 1993; Dale *et al*, 1995; Ching *et al*, 1996), we previously defined a core recognition motif on AMPK target proteins, that is, $\phi(X,\beta)XXS/TXXX\phi$, where ϕ and β are hydrophobic and basic residues, respectively, with S/T representing the phosphorylated serine or threonine. More recently (Scott *et al*, 2002), we identified additional specificity determinants outside of this core motif, especially another basic residue at the P-6 position (i.e. six residues N-terminal to the phosphoamino acid) and an amphipathic α -helix stretching from P-16 to P-5, with regularly spaced hydrophobic residues at P-16, P-13, P-9 and P-5, which would all lie on one face of the helix. According to a model of the AMPK kinase domain based on atomic coordinates of related protein kinases, this amphipathic α -helix fits into a deep hydrophobic groove on the large lobe of the kinase domain, a hypothesis supported by extensive site-directed mutagenesis (Scott *et al*, 2002) and by a recent crystal structure for the kinase domain of the yeast orthologue Snf1 (Rudolph *et al*, 2005). Figure 1 shows a sequence alignment of the sequence around Ser-79 on rat acetyl-CoA carboxylase-1 (ACC1, one of the best AMPK substrates) with part of the second CBS motif of the γ subunit isoforms of AMPK and the equivalent sequences in several other eukaryotic species. This reveals the presence of a putative pseudosubstrate sequence within the γ subunit that contains all of the residues in the extended recognition motif for AMPK, except that the phosphorylated serine is replaced by a non-phosphorylatable residue. In all γ subunit isoforms and all species examined, the position that would be occupied by the phosphoacceptor (labelled 'P' in Figure 1) has a hydrophobic residue instead (valine, leucine or isoleucine). In the full-length form of human $\gamma 2$, this residue is Val-387. In most cases, there are basic residues (underlined) at the P-3, P-4 and P-6 positions, and hydrophobic residues (bold type) at the P-16, P-13, P-9, P-5 and P+4 positions. We therefore set

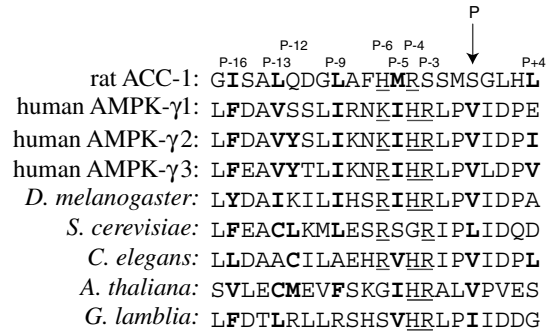


Figure 1 Alignment of the sequence around a known physiological AMPK phosphorylation site (Ser-79 on rat ACC1) with sequences of the putative pseudosubstrate sequences in the second CBS motif of AMPK/Snf1 γ subunits. The phosphorylation/pseudosubstrate site is marked with a vertical arrow and 'P'; basic residues at the P-3, P-4 and P-6 positions are underlined; hydrophobic residues at the P-16/P-13/P-9/P-5/P+4 positions are in bold type. Sequences of γ subunits (UniProt-SwissProt-TREMBL accession numbers/residue numbers in parentheses) were human $\gamma 1$ (P54619/138–159), human $\gamma 2$ (Q9UGJ0/370–391), human $\gamma 3$ (Q9UGI9/268–289), *Drosophila melanogaster* (O96613/279–300), *S. cerevisiae* (P12904/132–153), *Caenorhabditis elegans* (O02168/164–185), *Arabidopsis thaliana* (Q9XI37/135–156) and *Giardia lamblia* (Q7R5H3/139–160).

out to test the hypothesis that the region around Val-387 acts as an auto-inhibitory sequence that binds and inhibits the kinase domain on the α subunit in the absence of AMP.

The pseudosubstrate sequence acts as a potent competitive inhibitor of AMPK

As an initial test of our hypothesis, we cloned DNA encoding the putative pseudosubstrate sequence (residues 367–402 from the full-length form of human $\gamma 2$) and expressed it in *Escherichia coli*, using a vector we had previously designed to express the substrate sequence on rat ACC1. This vector provides a glutathione-S-transferase (GST) domain at the N-terminus separated from the insert by a polyglycine spacer and a His₆ tag at the C-terminus that inhibits degradation of the fusion protein in *E. coli* (Scott *et al*, 2002). The new fusion protein (GST- $\gamma 2$ -PS) could be purified on Ni²⁺-Sepharose with a good yield (8 mg/l of culture) and >95% purity as judged by SDS-PAGE. Figure 2A shows the effect of various concentrations of GST- $\gamma 2$ PS on the phosphorylation by AMPK of increasing concentrations of the SAMS peptide. The data were fitted to the Michaelis–Menten equation, which revealed that increasing concentrations of GST- $\gamma 2$ -PS increased the apparent K_m for the substrate peptide, without affecting V_{max} . A re-plot of the apparent K_m values against inhibitor concentration (Figure 2B) demonstrated that the pseudosubstrate peptide inhibited AMPK activity in a manner that was competitive with the SAMS peptide, with a K_i of $7.2 \pm 1.6 \mu\text{M}$. Determination of the apparent K_m for MgATP in the presence of increasing concentrations of GST- $\gamma 2$ -PS showed that inhibition by the latter was uncompetitive with respect to MgATP (not shown).

Mutation of the valine in the pseudosubstrate sequence to serine converts it into a good substrate

Next, we mutated the valine residue in GST- $\gamma 2$ -PS (equivalent to Val-387 in full-length $\gamma 2$) to the phosphorylatable residue serine. Unlike the parent fusion protein, this GST- $\gamma 2$ -PS-

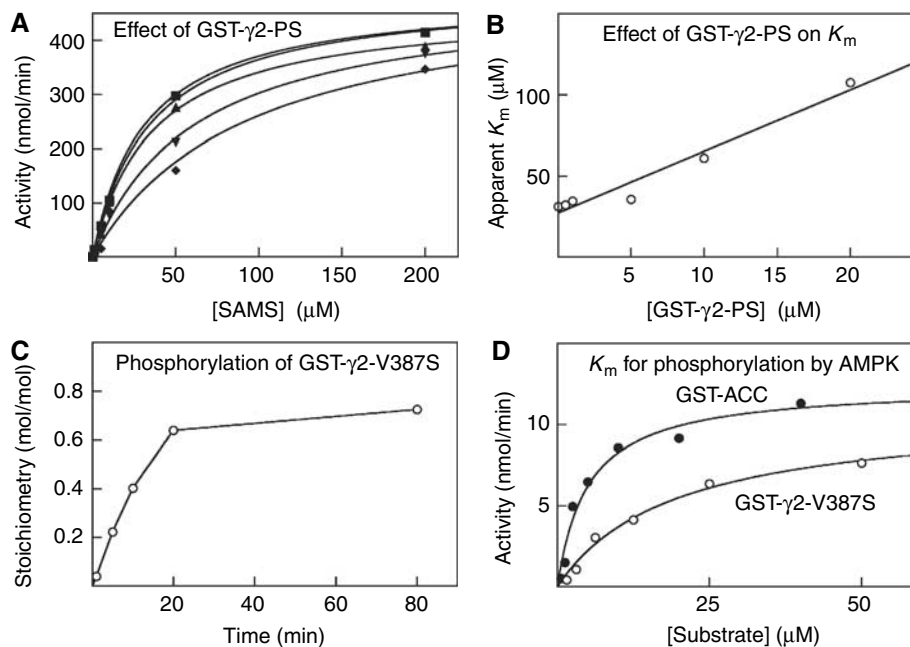


Figure 2 (A) Effect of increasing concentrations of GST-PS on the apparent K_m for the substrate peptide SAMS; (B) replot of apparent K_m against the concentration of GST-PS, using data from (A); (C) extent of phosphorylation of GST- γ 2-V387S protein as a function of time; (D) initial velocity of phosphorylation of GST- γ 2-V387S and GST-ACC (Scott *et al*, 2002) as a function of substrate concentration. In (A), the initial rate of phosphorylation of the SAMS peptide was determined at various concentrations of SAMS in the presence of increasing concentrations (μ M) of GST-PS ((●), 0; (■), 1; (▲), 5; (▼), 10; (◆), 20 μ M). In (A) and (D), data were fitted to the Michaelis-Menten equation using GraphPad Prism. In (B), the values for apparent K_m obtained from (A) were replotted against the concentration of the GST- γ 2-PS peptide.

V387S mutant was readily phosphorylated by AMPK with a stoichiometry approaching 1 mol/mol and a K_m of $19 \pm 4 \mu$ M (Figure 2C and D). This is comparable with the K_m for the substrate used in the standard AMPK assay, the SAMS peptide ($26 \pm 4 \mu$ M) (Dale *et al*, 1995), and that of the best model substrate based on the sequence of rat ACC1 ($5 \pm 1 \mu$ M; Figure 2D; Scott *et al*, 2002).

A V387S mutant of full-length γ 2 becomes phosphorylated in the heterotrimeric complex

If a V387S mutant in the context of the GST- γ 2-PS fusion protein was a good substrate for AMPK, one might expect the serine residue in a V387S mutant to become autophosphorylated in the intact AMPK complex. To test this, heterotrimeric α 1 β 1 γ 2 complexes containing wild-type γ 2 or a V387S mutant were expressed in HEK-293 cells and immunoprecipitated by means of the *myc* tag on the α 1 subunit. The complexes were allowed to autophosphorylate in the presence of [γ - 32 P]ATP, with or without AMP. Only a low level of phosphate incorporation was obtained, possibly because the protein had already been phosphorylated in the intact cells (unfortunately, protein phosphatase treatment cannot be used because this would inactivate the kinase). Nevertheless, the results revealed a faint autophosphorylation of a 63 kDa polypeptide in both the wild-type and mutant complexes (Figure 3A), with Western blot analysis confirming that this was the α 1 subunit (Figure 3B). Using the γ 2 V387S complex but not the wild-type γ 2 complex, an additional 32 P-labelled polypeptide of lower molecular mass was observed (Figure 3A), and Western blotting using anti-FLAG antibody to detect the tag on γ 2 confirmed that this was indeed the γ 2 subunit (Figure 3C). Intriguingly, the autophosphorylation of the γ 2 subunit was completely suppressed by AMP.

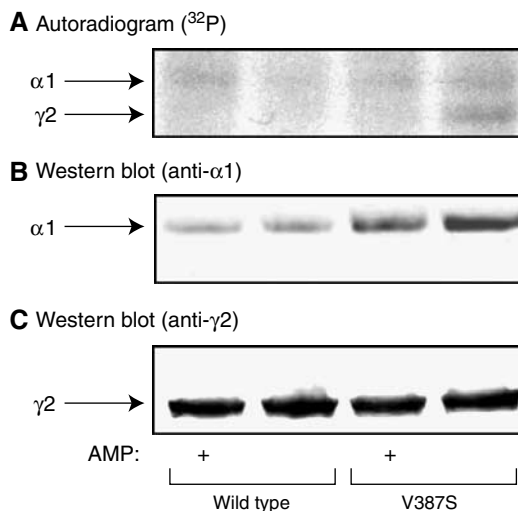


Figure 3 Recombinant α 1 β 1 γ 2 complexes containing a V387S mutation, but not the wild type (WT), autophosphorylate on the γ 2 subunit, and this is suppressed by AMP. Plasmids encoding WT or V387S mutant γ 2 subunit were coexpressed with α 1 and β 1 in CCL13 cells, and the recombinant complexes immunoprecipitated via the *myc* tag on α 1. The immunoprecipitate was incubated with $MgCl_2$ and [γ - 32 P]ATP in the presence and absence of 100 μ M AMP and analysed by SDS-PAGE followed by autoradiography (A) or Western blotting using anti- α 1 antibody (B) or anti-FLAG antibody (C).

Generation of partially activated α β γ 2 complexes by mutating residues around Val-387

As another test of our hypothesis, we mutated residues around Val-387 that we expected from our previous studies (Scott *et al*, 2002) would weaken the association between the

pseudosubstrate sequence and the kinase domain, and expressed them in HEK-293 cells. We expected that this would increase the basal activity of the complex in the absence of AMP. We mutated to alanine the hydrophobic residues at P-13 and P+4, as well as the basic residues at P-6, P-4 and P-3 (see Figure 1). We also made a double mutation of the basic residues at P-4 and P-3. The cells were initially harvested using the 'slow lysis' method (which leads to maximal phosphorylation of Thr-172 due to stresses during cell harvesting; Scott *et al*, 2004), after which we immunoprecipitated the recombinant protein using anti-myc antibody, and assayed in the presence and absence of AMP. This allowed us to test the effect of the mutations on allosteric activation by AMP, without the complicating factor of differing phosphorylation status. The results (Figure 4A) showed that, as predicted by our hypothesis, these mutations increased the basal activity of the complex in the absence of AMP, but did not affect the total activity in the presence of AMP. The basal activity seemed to be increased by all mutations to some extent, but particularly significant effects were seen with the mutations at P-13 and P-3, and the double P-4/P-3 mutants.

We also harvested the cells using a 'rapid lysis' procedure that we believe preserves the natural phosphorylation state of AMPK in the cells, and then measured the AMPK activity in the presence of AMP. This allowed us to test the effect of the mutations on the phosphorylation state of the protein in the cells independently of any effect on allosteric activation. Once again, the results showed that most of these mutations increased the basal activation state of AMPK, with the P-3 and the double P-4/P-3 mutations having the largest effect. This was associated with increased phosphorylation of the activating site, Thr-172, in the mutants as measured using a phosphospecific antibody (Figure 4B). The total amount of the $\alpha\beta\gamma$ complex recovered was the same with all mutants, as judged by Western blotting using anti- α 1 and anti- β 1 antibodies (Figure 4B).

To test the effects that these mutations had on AMP binding, we also introduced them into a vector that allows expression of the tandem Bateman domains from γ 2 as a GST fusion in *E. coli* (Scott *et al*, 2004). We tested their ability to bind [³H]AMP using a novel scintillation proximity assay, which has the advantage over our previous rapid filtration assay that it is not necessary to separate the bound and the free nucleotides. The wild-type γ 2 Bateman domains had a $B_{0.5}$ for AMP (concentration causing half-maximal binding) of $39 \pm 11 \mu\text{M}$, close to the value of $53 \pm 5 \mu\text{M}$ reported using the rapid filtration assay (Scott *et al*, 2004). For the P-13, P-4 and P-4/P-3 mutants, the $B_{0.5}$ values were 118 ± 47 , 50 ± 9 and $177 \pm 31 \mu\text{M}$, respectively. Thus, these mutations have only modest (1.3–4.5-fold) effects on the affinity for AMP. By contrast, the R531G and R531Q mutations, which affect the fourth CBS motif that lacks a pseudosubstrate sequence, increase the $B_{0.5}$ values by 50- and 100-fold, respectively (Scott *et al*, 2004; Burwinkel *et al*, 2005). Unfortunately, the GST fusions containing the P-3 and the P+4 mutations appeared to be insoluble and we could not determine AMP binding.

Pseudosubstrate mutations cause constitutive activation of the yeast homologue Snf1 *in vivo*

In the previous section, mutations that would be expected to weaken the interaction between the pseudosubstrate

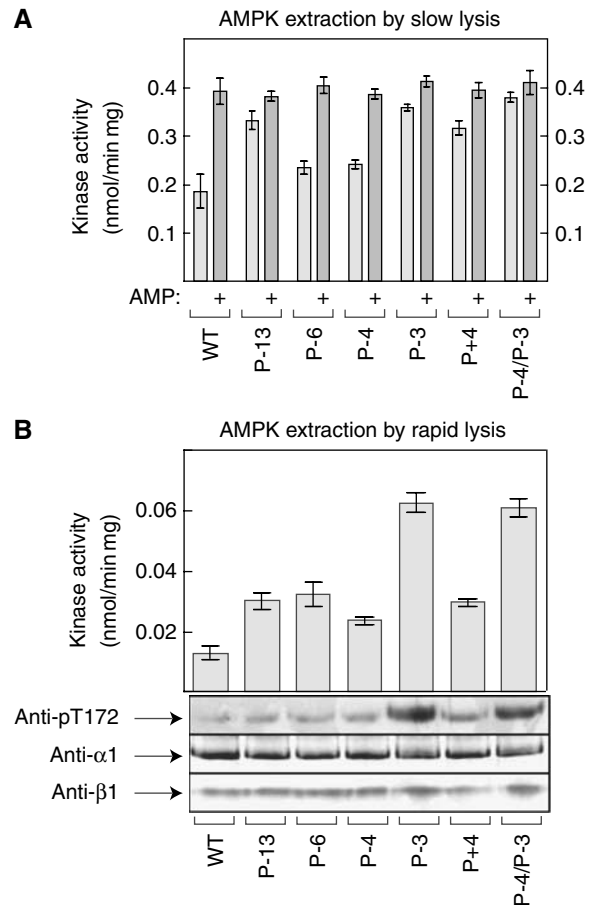


Figure 4 (A) allosteric activation by AMP and (B) basal activity and phosphorylation of recombinant AMPK (α 1 β 1 γ 2 complex) with either the wild-type (WT) γ 2 sequence or various mutation to alanine of residues within the pseudosubstrate sequence on γ 2. Labelling of positions within the pseudosubstrate sequence is as in Figure 1. In (A), the cells were harvested by the slow-lysis procedure, followed by immunoprecipitation with anti-myc antibody before assay in the presence and absence of 200 μM AMP. The slow-lysis procedure results in maximal phosphorylation of Thr-172, so that the effect of the mutations on allosteric activation by AMP could be studied, independently of any effects on phosphorylation of Thr-172. In (B), the cells were harvested by the rapid lysis procedure, which preserves the phosphorylation state of Thr-172 present in the intact cells. The assays of anti-myc immunoprecipitates were then conducted in the presence of 200 μM AMP (upper panel of (B)), so that the effect of the mutations on the activity of AMPK, due to varying basal phosphorylation of Thr-172 in the intact cells, could be observed independently of any allosteric effects. The bottom panels show Western blotting of the immunoprecipitates using anti-pT172 (a phosphospecific antibody dependent on phosphorylation of Thr-172) and anti- α 1 and - β 1 (which are phosphorylation-independent).

sequence and the kinase domain caused increases in the basal activity of AMPK in cultured cells, but we also wished to test these mutations *in vivo*. Making knock-in mutations in mice is feasible but time consuming. We therefore decided to mutate to alanine two of the pseudosubstrate residues that are conserved (see Figure 1) in the sequence of the yeast orthologue Snf4, that is, Leu-137 (P-12) and Arg-146 (P-3), and express these mutant or wild-type *SNF4* in a yeast strain deleted for the gene, using a plasmid with a low copy number. Unlike the parent *snf4*- Δ strain, the strains expressing these plasmids grew in the presence of raffinose (which

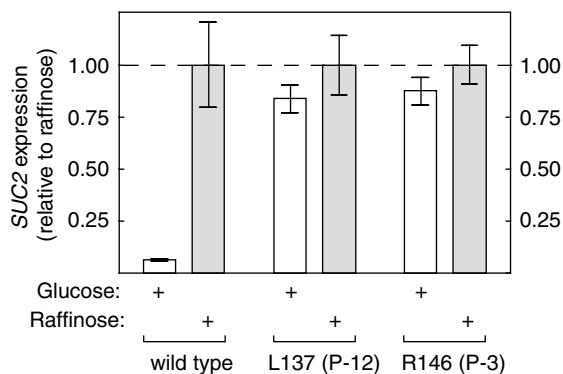


Figure 5 Expression of the *SUC2* gene measured by real-time PCR in yeast cells grown in glucose or raffinose. Cells deleted for *SNF4* (*snf4-Δ*) were transformed with plasmids encoding wild-type *SNF4* or L137A and R146A mutants. Results are expressed relative to the expression in raffinose for that strain. The absolute levels of expression of *SUC2* in the presence of raffinose were not markedly different between the three strains (in arbitrary units: wild type, 0.901 ± 0.184 ; L137A, 0.807 ± 0.074 ; R146A, 1.335 ± 0.189).

requires a functional complex between *Snf1*, *Snf4* and one of the three yeast β subunits (Schmidt and McCartney, 2000) to switch on *SUC2*, required for metabolism of raffinose), confirming that *SNF4* function had been restored. We then tested using real-time PCR whether expression of *SUC2* was repressed by glucose and induced by raffinose in these strains. Figure 5 shows that, in yeast expressing wild-type *SNF4*, this was indeed the case, with the expression of *SUC2* mRNA being > 10-fold higher in the presence of raffinose rather than glucose. However, using both the L137A and R146A mutants of *Snf4*, the expression of the *SUC2* gene was almost as great with glucose in the medium as with raffinose. This confirms that these mutations cause an increased basal activity of the *SNF1* complex *in vivo*.

Discussion

Our results provide strong support for the hypothesis that the pseudosubstrate sequences that we identified in the second CBS domain of the γ subunits of AMPK, and their orthologues in non-mammalian eukaryotic species such as *Saccharomyces cerevisiae* (Figure 1), act as auto-inhibitory sequences that bind to and block the substrate-binding groove on the α subunit in the absence of the activating ligand 5'-AMP. The evidence for this may be summarized as follows:

- (1) When this sequence was expressed in bacteria as a GST fusion, it acted as a potent inhibitor of AMPK, which was competitive with the *SAMS* substrate peptide, with a K_i of 7 μ M (Figure 2A and B).
- (2) When the valine in the GST fusion (occupying the position of the phosphorylated amino acid in a substrate) was mutated to a serine, the protein now became an excellent substrate for AMPK with a K_m of 19 μ M, comparable with that of the best-known substrates for AMPK (Figure 2C and D).
- (3) When this valine (Val-387) was mutated to a serine in full-length $\gamma 2$ and the subunit expressed in the context of a heterotrimeric $\alpha 1\beta 1\gamma 2$ AMPK complex, the $\gamma 2$ subunit became autophosphorylated on incubation of the complex with MgATP, which was not seen with the wild-type $\gamma 2$ sequence (Figure 3).

- (4) The autophosphorylation of the V387S mutant occurred only in the absence of AMP, suggesting that binding of the activating ligand prevents the interaction of this site with the α subunit (Figure 3).
- (5) When $\alpha 1\beta 1\gamma 2$ complexes were expressed in HEK-293 cells and extracted under conditions that caused maximal phosphorylation of Thr-172, mutations in residues around Val-387 on $\gamma 2$ that would be expected to weaken the pseudosubstrate interaction (particularly those at the P-13, P-3 and P-4/P-3 positions) led to $\alpha 1\beta 1\gamma 2$ complexes with increased activity in the absence of AMP, although the maximal activity in the presence of AMP was unchanged (Figure 4A). These mutations differ from the mutations that cause hereditary Wolff-Parkinson-White syndrome in humans (Daniel and Carling, 2002; Scott *et al*, 2004), in that they had only modest effects on the binding of AMP, and increased the activity in the absence of AMP rather than decreasing the activity in the presence of AMP.
- (6) When $\alpha 1\beta 1\gamma 2$ complexes were expressed in HEK-293 cells and extracted under conditions that preserve the phosphorylation status of Thr-172, the mutants had increased activity in the presence of AMP, and this was associated with increased phosphorylation of the activating site, Thr-172 (Figure 4B). This last result indicates that the pseudosubstrate sequence may not only inhibit the activity of AMPK in the absence of AMP, but also inhibit its phosphorylation by LKB1 in the absence of the nucleotide. However, this does not rule out the possibility that the mutations affect dephosphorylation.
- (7) Mutations in the yeast γ subunit *Snf4*, which would be expected to weaken the association between the auto-inhibitory sequence and the kinase domain on the α subunit, *Snf1*, led to constitutive activation of the *SNF1* complex *in vivo*, assessed by the failure of glucose to repress expression of *SUC2* (Figure 5).

According to the atomic model of the first Bateman domain of $\gamma 2$ that we constructed previously (Scott *et al*, 2004) (based on the coordinates of a related domain in a bacterial IMP dehydrogenase), the residues from the P-16 to the P-7 positions in the pseudosubstrate sequence form an α -helix (Figure 6), corresponding to helix $\alpha 1$ in the generic structure of CBS repeats (Ignoul and Eggermont, 2005). We had previously proposed that the residues from the P-16 to the P-5 positions in substrates for AMPK form an amphipathic α -helix (Scott *et al*, 2002), and such a helix was indeed observed in the crystal structure of one target protein, 3-hydroxy-3-methyl-CoA reductase (Istvan *et al*, 2000). Intriguingly, in our model for the first Bateman domain, the hydrophobic side chains at P-16 (Phe), P-13 (Val), P-12 (Tyr) and P-9 (Ile) point outwards from this α -helix, towards the solvent. They would thus be readily available for binding in the hydrophobic groove on the large lobe of the α subunit kinase domain (Scott *et al*, 2004). However, from P-6 to P-4, there is a sharp turn, followed by a β strand running in the reverse direction from Arg-384 (P-3) to Val-387 (the pseudosubstrate residue itself). This β strand ($\beta 1$), together with the antiparallel $\beta 2$ strand that follows it, forms the central β sheet in the second CBS motif that (in bacterial IMP dehydrogenase) associates via hydrophobic interactions with the equivalent β sheet from the first CBS motif to complete a β -sandwich

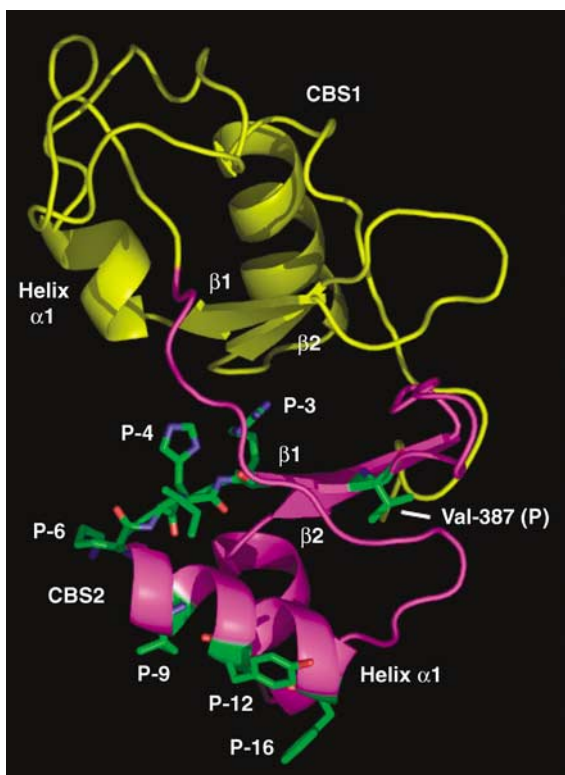


Figure 6 View of a model of the CBS1–CBS2 Bateman domain of $\gamma 2$ (Scott *et al*, 2004) displayed using PyMol (DeLano Scientific). CBS1 is in yellow and CBS2 in magenta. The model is in ‘cartoon’ representation except that the side chains of the residues at the P-16, P-12, P-9, P-6, P-5, P-4 and P-3 positions in the pseudosubstrate sequence, and of Val-387 (P), are represented in ‘stick’ representation. Labelling of positions within the pseudosubstrate sequence is as shown in Figure 1. For these residues, carbon atoms are in green, nitrogen in blue and oxygen in red; hydrogen atoms are omitted. The positions of helix $\alpha 1$ and strands $\beta 1$ and $\beta 2$ in CBS1 and CBS2 are indicated.

structure. We propose that the adenosine moieties of AMP or ATP are accommodated within the hydrophobic cleft formed at one end of this β -sandwich, with their α -phosphates interacting with the basic side chains at the mouth of the cleft (Scott *et al*, 2004). In the second CBS motif, these basic side chains are located at the P-3 and P-4 positions in the pseudosubstrate sequence. According to alignments of CBS motifs in the Pfam database (Bateman *et al*, 2002) (www.sanger.ac.uk/software/pfam/), a hydrophobic residue at the position occupied by Val-387 is conserved in almost all CBS motifs, as is the hydrophobic residue at the P-13 position. However, the hydrophobic residues at the P-16, P-9, P-5 and P + 4 positions, and the basic residues at the P-3, P-4 and P-6 positions, are not conserved in CBS motifs from other proteins. This suggests that the conservation of these residues in the second CBS motif of the γ subunits of AMPK (and its orthologues in non-mammalian eukaryotes) is not simply a consequence of the necessity to form the Bateman domain fold. This is also evident from the fact that a potential pseudosubstrate sequence is not present in the first, third or fourth CBS motif of the AMPK γ subunits.

In our structural model (Figure 6), the side chain of Val-387 is almost completely inaccessible to solvent and, if the Bateman domain adopted this conformation, Val-387 would clearly not be available to form an interaction with the

substrate-binding groove on the α subunit. This suggests to us a likely mechanism whereby AMP activates the AMPK complex. We propose that, in the absence of AMP, the C-terminal Bateman domain (formed by the third and fourth CBS motifs, which we shall term domain B) is folded into a conformation similar to that in Figure 6, but that the N-terminal domain (formed by the first and second CBS motifs, which we shall term domain A) is partially unfolded. In this state, domain A would have little or no affinity for AMP. However, the full pseudosubstrate sequence from P-16 to P + 4 in the second CBS motif (including the pseudosubstrate residue itself, Val-387) would be available to bind in the substrate-binding groove on the kinase domain of the α subunit, thus blocking access both to the upstream kinase, LKB1, and to downstream target proteins. We next propose that initial binding of AMP to domain B promotes the folding of domain A into a unit more capable of binding the nucleotide. Subsequent binding of AMP to domain A, which would produce the fully folded conformation similar to that shown in Figure 6, would weaken or prevent the interaction of the pseudosubstrate sequence with the α subunit. This would occur both because the sharp turn between helix $\alpha 1$ (P-17 to P-7) and strand $\beta 1$ (P-3 to Val-387) would preclude full binding to the substrate-binding groove, but also because in our model, the basic residues at the P-4/P-3 positions make interactions either with an acidic patch on the kinase domain (Scott *et al*, 2002) or with the phosphate group of AMP (Scott *et al*, 2004). Clearly, they could not do both at the same time, so that interaction with the kinase domain or with AMP would be mutually exclusive. Thus, when AMP binds to domain A, the α and γ subunits would partially or completely dissociate, exposing Thr-172 for phosphorylation by the LKB1 complex, although the two subunits would still remain tethered via the β subunit. Once Thr-172 was phosphorylated, the active site would then be available for phosphorylation of downstream target proteins. Although this is currently only a working model and will require detailed structural studies for verification, there is some existing evidence that supports it:

- (1) A bacterially expressed construct containing both Bateman domains from $\gamma 2$ binds two molecules of AMP with strong positive cooperativity (Hill coefficient ≈ 2) (Scott *et al*, 2004). This cooperativity could be explained if binding of AMP to domain B promotes the folding of domain A.
- (2) In the heterotrimeric complex containing the V387S mutant, the $\gamma 2$ subunit becomes autophosphorylated, but only in the absence of AMP (Figure 3A). This rather unusual finding of an AMP-inhibited phosphorylation by AMPK can be explained by our proposal that AMP binding promotes the complete folding of domain A, resulting in a conformation in which Val-387 (or in this mutant, Ser-387) would be in an inaccessible location in the centre of the domain.
- (3) The fact that $\gamma 2$ mutations in both domain A (R302Q, H383R, T400N) and domain B (N488I, R531G, R531Q) cause heart disease in humans *in vivo*, as well as interfere with activation of AMPK by AMP *in vitro* (Daniel and Carling, 2002; Scott *et al*, 2004; Burwinkel *et al*, 2005), suggests that both sites must be occupied to allow activation. Four of these mutations affect basic residues (R302, H383 and R531) that occupy equivalent positions

in the first, second and fourth CBS motifs, and we have proposed that these are involved in binding the phosphate group of AMP (Scott *et al*, 2004). The R531G and R531Q mutations have a particularly severe effect in that they generate completely AMP-insensitive complexes. In our model, the initial binding of AMP occurs at domain B, which then promotes binding at domain A. Mutations that affect the initial binding site are more likely to have a severe effect.

As well as explaining allosteric activation by AMP, our model can also potentially explain why AMP binding to AMPK promotes the phosphorylation of Thr-172 by the upstream kinase LKB1 via a substrate-mediated effect (Hawley *et al*, 1995, 2003). In our model of the α 1-kinase domain based on homology with related kinases (Scott *et al*, 2002), Thr-172 lies very close to the position occupied by the P+4 residue of the protein substrate, and it is easy to see how binding of the full pseudosubstrate sequence might cause steric hindrance of phosphorylation of Thr-172. A difficulty with this is that AMP does not appear to stimulate phosphorylation of Thr-172 by the alternate upstream kinase CaMKK β (Hawley *et al*, 2005). An alternative model is that the dissociation of the α and γ subunit may expose a previously hidden docking site for LKB1 that is not required for phosphorylation by CaMKK β .

Another feature not addressed by our current model is why AMP binding to AMPK inhibits dephosphorylation of Thr-172, which we have observed experimentally (Davies *et al*, 1995). One can envisage models in which the folded conformation of domain A, with bound AMP, promotes the stability of interactions between the phosphorylated form of Thr-172 and other side chains such that it is shielded from protein phosphatases. However, more detailed structural analysis of AMPK complexes may be required before testable predictions can be made.

It has not escaped our notice that our proposed mechanism of activation of AMPK by AMP bears striking similarities to the proposed mechanism by which binding of cyclic AMP to the regulatory subunits activates cyclic AMP-dependent protein kinase (PKA). The regulatory subunit isoforms of PKA (Su *et al*, 1995; Diller *et al*, 2001) contain an N-terminal dimerization domain followed by a linker region containing a pseudosubstrate sequence (RI isoform) or an autophosphorylation site (RII isoform). These are followed by two tandemly repeated cyclic AMP-binding domains (domains A and B). Cyclic AMP is believed to bind initially to the C-terminal domain (domain B), and the associated conformational change in domain B is thought to increase the affinity of domain A for the cyclic nucleotide. Cyclic AMP binding at domain A then prevents the interaction of the pseudosubstrate sequence or autophosphorylation site with the catalytic subunit. Although the cyclic AMP-binding domains of PKA and the AMP-binding domains of AMPK are not obviously related in sequence, it is intriguing that a similar mechanism, which promotes a switch-like activation of both AMPK and PKA, appears to have evolved independently, that is, via convergent evolution.

Finally, it is important to reconcile our results with a proposed mechanism for the regulation of AMPK and its yeast orthologue, the SNF1 complex, that at first sight might look rather different from our model. Crute *et al*

(1998) expressed in COS7 cells a truncated construct comprising residues 1–392 of rat α 1, and found that it displayed low activity compared with a construct comprising residues 1–312, which is truncated close to the C-terminal end of the kinase domain. They therefore suggested that the region from 312 to 392 contained an auto-inhibitory domain (AID). Very recently, Pang *et al* (2007) have made further truncations to narrow this putative AID down to a sequence from residues 313 to 335. Unlike the γ 2 sequence defined in this paper, the AID does not contain a discernible pseudosubstrate, and does not inhibit kinase activity (Pang *et al*, 2007). These authors also modelled the binding of the proposed AID to the kinase domain, based on a crystal structure of the AMPK-related kinase MARK2, and suggested that it formed an α -helix bundle that bound to the small lobe of the kinase domain, on the opposite face to the substrate-binding groove. The AID defined by Pang *et al* is highly conserved within vertebrates, but is less well conserved between vertebrates and *S. cerevisiae*. Nevertheless, a variety of evidence obtained from studies of the yeast SNF1 complex also support a role for an AID in the C-terminal region of the α subunit:

- (1) In genetic studies, the yeast γ subunit gene, *SNF4*, behaves as an activator rather than an inhibitor of the SNF1 complex. For example, deletion of *SNF4* leads to loss of function, but this can be partially alleviated by increased dosage of the gene encoding the α subunit (*SNF1*) or by deletion of the C-terminal region of the latter (Celenza and Carlson, 1989). These results suggested that the C-terminal region of the α subunit contains an AID whose effect can be relieved by the γ subunit.
- (2) Two-hybrid analysis suggested that in low glucose (when the SNF1 complex is active), the yeast γ subunit (Snf4) interacts with the C-terminal domain of the α subunit (Snf1) (Jiang and Carlson, 1996). By contrast, in high glucose (when the SNF1 complex is inactive), the α subunit C-terminal domain appeared to interact not with the γ subunit, as suggested by our model, but with the kinase domain. The latter could correspond to the interaction between the putative AID in the C-terminal region and the kinase domain.
- (3) A strain expressing mutant Snf1 with a deletion in the C-terminal domain (381–488, containing the region equivalent to the proposed AID on mammalian α 1), but not full-length Snf1, was able to grow on raffinose even in the absence of Snf4 (Leech *et al*, 2003). Surprisingly, the downstream target gene *SUC2* (required for growth on raffinose) was still induced by glucose starvation in this strain, albeit to a lesser extent than in a strain expressing wild-type Snf1 and Snf4. This suggests that there is a mechanism for activation of the SNF1 complex during glucose starvation in yeast that requires neither the putative AID on the α subunit nor Snf4.
- (4) Leech *et al* (2003) also screened for point mutations in Snf1 that would grow on raffinose in the absence of the γ subunit (Snf4). Interestingly, the four mutations found affected residues that are all located on the large lobe of the kinase domain. In the published crystal structure (Nayak *et al*, 2006), two of them are buried, but the other two (Tyr-167 and Lys-192) are exposed on the surface on the opposite face from the substrate-binding groove. This may represent the binding site for the

proposed AID on the C-terminal region of the α subunit, although it is slightly different from the binding site proposed for the AID on mammalian $\alpha 1$, which was on the small lobe.

- (5) When expressed in yeast cells lacking β and γ subunits, full-length Snf1 had a lower activity than the kinase domain, but could be stimulated by addition of β and γ subunits *in vitro* (Elbing *et al*, 2006). This is different from results in the mammalian system, because the mammalian α subunits appear to be very unstable in the absence of β and γ , whether expressed in mammalian cells (Dyck *et al*, 1996; Woods *et al*, 1996) or bacteria (Neumann *et al*, 2003), and all attempts to reconstitute the complex by mixing free subunits in cell-free assays have failed. Nevertheless, it is consistent with the idea that the C-terminal region of the α subunit contains an AID whose effect can be relieved by the binding of the γ subunit.

Can these results be reconciled with our model? We think that they can, because our model does not rule out the possibility that there is an AID in the C-terminal domain of the α subunit that inhibits the kinase domain in concert with our proposed pseudosubstrate sequence. The binding sites for the AID suggested by the studies of Leech *et al* (2003) for the yeast complex and Pang *et al* (2007) for the mammalian enzyme, although slightly different, are both on the opposite face of the kinase domain to the substrate-binding groove. This means that it would be perfectly feasible for our pseudosubstrate sequence from $\gamma 2$ to be bound to the kinase domain at the same time, and to inhibit the kinase in concert with the AID on the α subunit. When AMP binds to domain A, as well as causing dissociation of the pseudosubstrate sequence on α from the substrate-binding groove on γ , there may also be a conformational change that relieves the inhibitory effect of the AID on kinase activity.

An interaction between the γ subunit (Snf4) and the kinase domain of Snf1, as proposed by our model, has not been detected by two-hybrid analysis in the yeast system, possibly because it is not sufficiently stable unless the β subunit is also present. However, the high degree of conservation of the pseudosubstrate sequence between eukaryotic species (Figure 1) and the finding that mutation of this sequence in yeast leads to constitutive expression of the *SUC2* gene (Figure 5) suggest that the pseudosubstrate sequence on γ may be important in the regulation of the SNF1 complex as well as the AID on Snf1. Surprisingly, the data of Leech *et al* (2003) suggest that there is an additional mechanism for glucose regulation of the SNF1 complex that requires neither the AID on Snf1 nor the γ subunit Snf4. This may perhaps involve the protein phosphatase Reg1:Glc7 (Sanz *et al*, 2000), and whether a similar mechanism exists in the mammalian system is unclear at present. Ultimately, protein structural data will be required to resolve all of the obvious complexities of the regulation of the AMPK and SNF1 complexes.

Materials and methods

PCR primers

The following oligonucleotides were used as PCR primers or hybridization probes during this study:

- A: 5'-CGGAATTCGGCAAGCCTCTTCGATGCTGTA-3'
B: 5'-CGGGGTACCCCGCTTTGTGGGTAAGTCTATAAAG-3'

- C: 5'-GTTGGATCCTTCAATGGTACT-3'
D: 5'-CCGTAGGTGGGTCAGTGTG-3'
E: 5'-ACTGAAGCTCCAATGAACCCATAATCATCAAAC-3'
F: 5'-GTAAATGGAACGAGGTGAGTAACACCATC-3'
G: 5'-CAAGGCATAGTAGTCCTTACCAAAATCTACCACCTC-3'
H: 5'-CTTCTACGTTTCCATCCAAGCCGTTTGTCTCTT-3'

DNA cloning and mutagenesis

DNA encoding the $\gamma 2$ pseudosubstrate sequence (residues 367–402) was isolated using the Stratagene *Pfu* Turbo PCR Kit with oligonucleotides A and B as primers and a pCDNA3 plasmid encoding human $\gamma 2$ as the template. The primers were designed with 5'-*Eco*RI and 3'-*Kpn*I sites to allow subsequent insertion of the amplified product into the bacterial expression plasmid, pGEX-KG. Mutations were generated using the Stratagene QuickChange Site-directed mutagenesis system.

Bacterial expression

LB medium (1 l) containing carbenicillin (50 μ g/ml) was inoculated with 10 ml of BL21 (DE3) *E. coli* culture containing the appropriate plasmid, and grown at 37°C until A_{600} reached 0.4. The culture was then induced with IPTG (1 mM) and the cells harvested 3 h later by centrifugation. The pellet was resuspended in 20 ml of lysis buffer (50 mM sodium phosphate pH 7.4, 500 mM NaCl, 10 mM imidazole) containing 1 mg/ml lysozyme and complete protease inhibitor cocktail (Roche). After incubation on ice for 30 min, the cells were lysed in *N*-octylglucoside (2% v/v) and the suspension was subsequently clarified by ultracentrifugation at 300 000 g for 1 h at 4°C. The cleared lysate was applied to a 5 ml Chelating-Sepharose column charged with 50 mM NiSO₄ and pre-equilibrated with 5 column volumes of lysis buffer. The column was washed with 10 volumes of lysis buffer containing 200 mM imidazole. Protein was eluted with 500 mM imidazole and detected with the Bradford assay and SDS-PAGE analysis. Pooled fractions were dialysed against 50 mM Hepes pH 7.4 and 1 mM DTT and concentrated using centrifugal ultrafiltration.

Cell culture

HEK-293 cells were grown in DMEM supplemented with 10% fetal bovine serum at 37°C in 5% CO₂. Plasmids encoding myc-tagged $\alpha 1$ and $\beta 1$ and FLAG-tagged $\gamma 2$ were purified using the QIAGEN HiSpeed Plasmid Maxi kits and expressed by transient transfection in HEK-293 cells. AMPK activities were determined by immunoprecipitation using anti-myc antibody and assayed as described previously (Scott *et al*, 2004).

Autophosphorylation of V387S mutant

Wild-type $\gamma 2$ and the V387S mutant were coexpressed by transient transfection with $\alpha 1$ and $\gamma 1$ in HEK-293 cells and immunoprecipitated with anti-myc antibody making use of the myc tag on $\alpha 1$ (Hardie *et al*, 2000; Scott *et al*, 2004). A reaction (25 μ l) containing 10 μ l of resuspended immunoprecipitate, MgCl₂ (5 mM) and [γ -³²P]ATP (200 μ M, 4 mCi/nmol), with or without AMP (100 μ M), was incubated for 1 h at 30°C in a rotary shaker. Reactions were terminated by the addition of 4 \times LDS sample buffer and samples resolved on a 4–12% Bis-Tris polyacrylamide gel in MES buffer (Invitrogen). The gel was either dried and subjected to autoradiography, or transferred to nitrocellulose. The membrane was incubated in Li-Cor Odyssey blocking buffer (Li-Cor Biosciences) for 1 h, then blocking buffer with Tween 20 (0.2% v/v) and either mouse anti-myc (Roche) or mouse anti-FLAG M2 (1 μ g/ml; Sigma) with gentle shaking for 2 h. The membrane was washed 6 \times 5 min with TBS-Tween (Tris-HCl, 10 mM, pH 7.4, 0.5 M NaCl, Tween-20 (0.2% v/v)), then in blocking buffer plus Tween-20 (0.2% v/v) and mouse IgG conjugated to IR-Dye 680 (1 μ g/ml; Molecular Probes) for 1 h. The membrane was washed 6 \times 5 min with TBS-Tween and 1 \times 5 min in water, and was scanned in the 700 nm channel using the Li-Cor Odyssey IR imager.

Bacterial expression of Bateman domains and measurement of AMP binding

Bacterial expression of GST fusions with CBS domains 1–4 of human $\gamma 2$, and site-directed mutagenesis, was as described previously (Scott *et al*, 2004). GST fusions were purified using a 5 ml GST FF column (GE Healthcare). The eluate was concentrated using a Vivapore (10/20, 30 kDa cutoff, Sartorius) and applied to a Superdex-200 size-exclusion column (GE Healthcare). Purified

protein was incubated with glutathione-coupled scintillation proximity assay (SPA) yttrium silicate beads (GE Healthcare), pre-blocked with 5% gelatin from cold-water fish skin (Sigma). The beads were washed with 50 mM Hepes pH 7.4, 200 mM NaCl and 1 mM DTT and resuspended to 10 mg/ml. A 96-well plate was set up with varying concentrations of [³H]AMP and 0.1 mg SPA beads, and made up to a final volume of 100 μ l with buffer. The plate was gently shaken for 15 min, beads allowed to settle and the plate was read using a 1450 Microbeta (Perkin-Elmer).

Transformation of yeast strains and analysis by real-time PCR

S. cerevisiae strain AY925 lacking SNF4 (*snf4* Δ) was transformed with YCPlac22 plasmid containing either the wild-type SNF4 gene (including its endogenous promoter and 5' and 3' regulatory elements) or the R146A (P-3) and L137A (P-12) pseudosubstrate mutants. Cultures were grown in YP medium supplemented with either 2% glucose or 2% raffinose plus 1 μ g/ml antimycin, at 30°C until they reached a density of $\approx 2 \times 10^7$ cells/ml. Total RNA was

extracted using the QIAGEN RNeasy Mini Kit. Real-time RT-PCR was performed using an ABI-PRISM 7000 Sequence Detection System and the TaqMan Gold RT-PCR kit (Applied Biosystems). The *SUC2* transcript was detected using the primers C and D. The *ACT1* transcript was used as an endogenous control and was detected using primers E and F. Fluorescent probes designed to hybridize with the amplified sequences were oligonucleotides G (*SUC2*) and H (*ACT1*) conjugated with TAMRA and JOE fluorescent dyes at their 5' and 3' ends, respectively.

Acknowledgements

This study was supported by the EXGENESIS Integrated Project (LSHM-CT-2004-005272) of the European Commission and a Programme Grant from the Wellcome Trust. FAR was supported by a BBSRC studentship and AstraZeneca, and JKDL by a Prize Studentship from the Wellcome Trust.

References

- Bateman A (1997) The structure of a domain common to archaeobacteria and the homocystinuria disease protein. *Trends Biochem Sci* **22**: 12–13
- Bateman A, Birney E, Cerruti L, Durbin R, Etmiller L, Eddy SR, Griffiths-Jones S, Howe KL, Marshall M, Sonnhammer EL (2002) The Pfam protein families database. *Nucleic Acids Res* **30**: 276–280
- Burwinkel B, Scott JW, Buhner C, van Landeghem FK, Cox GF, Wilson CJ, Hardie DG, Kilimann MW (2005) Fatal congenital heart glycogenosis caused by a recurrent activating R531Q mutation in the $\gamma 2$ subunit of AMP-activated protein kinase (PRKAG2), not by phosphorylase kinase deficiency. *Am J Hum Genet* **76**: 1034–1049
- Celenza JL, Carlson M (1989) Mutational analysis of the *Saccharomyces cerevisiae* SNF1 protein kinase and evidence for functional interaction with the SNF4 protein. *Mol Cell Biol* **9**: 5034–5044
- Cheung PCF, Salt IP, Davies SP, Hardie DG, Carling D (2000) Characterization of AMP-activated protein kinase γ subunit isoforms and their role in AMP binding. *Biochem J* **346**: 659–669
- Ching YP, Davies SP, Hardie DG (1996) Analysis of the specificity of the AMP-activated protein kinase by site-directed mutagenesis of bacterially expressed 3-hydroxy 3-methylglutaryl-CoA reductase, using a single primer variant of the unique site elimination (USE) method. *Eur J Biochem* **237**: 800–808
- Corton JM, Gillespie JG, Hawley SA, Hardie DG (1995) 5-Aminoimidazole-4-carboxamide ribonucleoside: a specific method for activating AMP-activated protein kinase in intact cells? *Eur J Biochem* **229**: 558–565
- Crute BE, Seefeld K, Gamble J, Kemp BE, Witters LA (1998) Functional domains of the alpha1 catalytic subunit of the AMP-activated protein kinase. *J Biol Chem* **273**: 35347–35354
- Dale S, Wilson WA, Edelman AM, Hardie DG (1995) Similar substrate recognition motifs for mammalian AMP-activated protein kinase, higher plant HMG-CoA reductase kinase-A, yeast SNF1, and mammalian calmodulin-dependent protein kinase I. *FEBS Lett* **361**: 191–195
- Daniel TD, Carling D (2002) Functional analysis of mutations in the $\gamma 2$ subunit of AMP-activated protein kinase associated with cardiac hypertrophy and Wolff-Parkinson-White syndrome. *J Biol Chem* **277**: 51017–51024
- Davies SP, Helps NR, Cohen PTW, Hardie DG (1995) 5'-AMP inhibits dephosphorylation, as well as promoting phosphorylation, of the AMP-activated protein kinase. Studies using bacterially expressed human protein phosphatase-2C α and native bovine protein phosphatase-2A α . *FEBS Lett* **377**: 421–425
- Diller TC, Madhusudan Xuong NH, Taylor SS (2001) Molecular basis for regulatory subunit diversity in cAMP-dependent protein kinase: crystal structure of the type II beta regulatory subunit. *Structure (Camb)* **9**: 73–82
- Dyck JRB, Gao G, Widmer J, Stapleton D, Fernandez CS, Kemp BE, Witters LA (1996) Regulation of the 5'-activated protein kinase activity by the noncatalytic β and γ subunits. *J Biol Chem* **271**: 17798–17803
- Elbling K, Rubenstein EM, McCartney RR, Schmidt MC (2006) Subunits of the SNF1 kinase heterotrimer show interdependence for association and activity. *J Biol Chem* **281**: 26170–26180
- Fryer LG, Parbu-Patel A, Carling D (2002) The anti-diabetic drugs rosiglitazone and metformin stimulate AMP-activated protein kinase through distinct pathways. *J Biol Chem* **277**: 25226–25232
- Goldberg J, Nairn AC, Kuriyan J (1996) Structural basis for the autoinhibition of calcium/calmodulin-dependent protein kinase I. *Cell* **84**: 875–887
- Hardie DG (2004) The AMP-activated protein kinase pathway—new players upstream and downstream. *J Cell Sci* **117**: 5479–5487
- Hardie DG, Sakamoto K (2006) AMPK: a key sensor of fuel and energy status in skeletal muscle. *Physiology (Bethesda)* **21**: 48–60
- Hardie DG, Salt IP, Davies SP (2000) Analysis of the role of the AMP-activated protein kinase in the response to cellular stress. *Methods Mol Biol* **99**: 63–75
- Hardie DG, Salt IP, Hawley SA, Davies SP (1999) AMP-activated protein kinase: an ultrasensitive system for monitoring cellular energy charge. *Biochem J* **338**: 717–722
- Hardie DG, Scott JW, Pan DA, Hudson ER (2003) Management of cellular energy by the AMP-activated protein kinase system. *FEBS Lett* **546**: 113–120
- Hawley SA, Boudeau J, Reid JL, Mustard KJ, Udd L, Makela TP, Alessi DR, Hardie DG (2003) Complexes between the LKB1 tumor suppressor, STRAD α/β and MO25 α/β are upstream kinases in the AMP-activated protein kinase cascade. *J Biol* **2**: 28
- Hawley SA, Pan DA, Mustard KJ, Ross L, Bain J, Edelman AM, Frenguelli BG, Hardie DG (2005) Calmodulin-dependent protein kinase kinase-beta is an alternative upstream kinase for AMP-activated protein kinase. *Cell Metab* **2**: 9–19
- Hawley SA, Selbert MA, Goldstein EG, Edelman AM, Carling D, Hardie DG (1995) 5'-AMP activates the AMP-activated protein kinase cascade, and Ca²⁺/calmodulin the calmodulin-dependent protein kinase I cascade, via three independent mechanisms. *J Biol Chem* **270**: 27186–27191
- Hurley RL, Anderson KA, Franzone JM, Kemp BE, Means AR, Witters LA (2005) The Ca²⁺/calmodulin-dependent protein kinase kinases are AMP-activated protein kinase kinases. *J Biol Chem* **280**: 29060–29066
- Ignoul S, Eggermont J (2005) CBS domains: structure, function, and pathology in human proteins. *Am J Physiol Cell Physiol* **289**: C1369–C1378
- Istvan ES, Palnitkar M, Buchanan SK, Deisenhofer J (2000) Crystal structure of the catalytic portion of human HMG-CoA reductase: insights into regulation of activity and catalysis. *EMBO J* **19**: 819–830
- Jiang R, Carlson M (1996) Glucose regulates protein interactions within the yeast SNF1 protein kinase complex. *Genes Dev* **10**: 3105–3115
- Kemp BE (2004) Bateman domains and adenosine derivatives form a binding contract. *J Clin Invest* **113**: 182–184
- Kemp BE, Parker MW, Hu S, Tiganis T, House C (1994) Substrate and pseudosubstrate interactions with protein kinases: determinants of specificity. *Trends Biochem Sci* **19**: 440–444

- Leech A, Nath N, McCartney RR, Schmidt MC (2003) Isolation of mutations in the catalytic domain of the Snf1 kinase that render its activity independent of the Snf4 subunit. *Eukaryot Cell* **2**: 265–273
- Minokoshi Y, Kim YB, Peroni OD, Fryer LG, Muller C, Carling D, Kahn BB (2002) Leptin stimulates fatty-acid oxidation by activating AMP-activated protein kinase. *Nature* **415**: 339–343
- Nayak V, Zhao K, Wyce A, Schwartz MF, Lo WS, Berger SL, Marmorstein R (2006) Structure and dimerization of the kinase domain from yeast Snf1, a member of the Snf1/AMPK protein family. *Structure* **14**: 477–485
- Neumann D, Woods A, Carling D, Wallimann T, Schlattner U (2003) Mammalian AMP-activated protein kinase: functional, heterotrimeric complexes by co-expression of subunits in *Escherichia coli*. *Protein Expr Purif* **30**: 230–237
- Pang T, Xiong B, Li JY, Qiu BY, Jin GZ, Shen JK, Li J (2007) Conserved alpha helix acts as autoinhibitory sequence in AMP-activated protein kinase alpha subunits. *J Biol Chem* **282**: 495–506
- Rudolph MJ, Amodeo GA, Bai Y, Tong L (2005) Crystal structure of the protein kinase domain of yeast AMP-activated protein kinase Snf1. *Biochem Biophys Res Commun* **337**: 1224–1228
- Saha AK, Avilucea PR, Ye JM, Assifi MM, Kraegen EW, Ruderman NB (2004) Pioglitazone treatment activates AMP-activated protein kinase in rat liver and adipose tissue *in vivo*. *Biochem Biophys Res Commun* **314**: 580–585
- Salt IP, Celler JW, Hawley SA, Prescott A, Woods A, Carling D, Hardie DG (1998) AMP-activated protein kinase—greater AMP dependence, and preferential nuclear localization, of complexes containing the $\alpha 2$ isoform. *Biochem J* **334**: 177–187
- Sanz P, Alms GR, Haystead TA, Carlson M (2000) Regulatory interactions between the Reg1-Glc7 protein phosphatase and the Snf1 protein kinase. *Mol Cell Biol* **20**: 1321–1328
- Schmidt MC, McCartney RR (2000) β -Subunits of Snf1 kinase are required for kinase function and substrate definition. *EMBO J* **19**: 4936–4943
- Scott JW, Hawley SA, Green KA, Anis M, Stewart G, Scullion GA, Norman DG, Hardie DG (2004) CBS domains form energy-sensing modules whose binding of adenosine ligands is disrupted by disease mutations. *J Clin Invest* **113**: 274–284
- Scott JW, Norman DG, Hawley SA, Kontogiannis L, Hardie DG (2002) Protein kinase substrate recognition studied using the recombinant catalytic domain of AMP-activated protein kinase and a model substrate. *J Mol Biol* **317**: 309–323
- Shaw RJ, Kosmatka M, Bardeesy N, Hurley RL, Witters LA, DePinho RA, Cantley LC (2004) The tumor suppressor LKB1 kinase directly activates AMP-activated kinase and regulates apoptosis in response to energy stress. *Proc Natl Acad Sci USA* **101**: 3329–3335
- Shaw RJ, Lamia KA, Vasquez D, Koo SH, Bardeesy N, Depinho RA, Montminy M, Cantley LC (2005) The kinase LKB1 mediates glucose homeostasis in liver and therapeutic effects of metformin. *Science* **310**: 1642–1646
- Su Y, Dostmann WR, Herberg FW, Durick K, Xuong NH, Ten Eyck L, Taylor SS, Varughese KI (1995) Regulatory subunit of protein kinase A: structure of deletion mutant with cAMP binding domains. *Science* **269**: 807–813
- Tomas E, Tsao TS, Saha AK, Murrey HE, Zhang CC, Itani SI, Lodish HF, Ruderman NB (2002) Enhanced muscle fat oxidation and glucose transport by ACRP30 globular domain: acetyl-CoA carboxylase inhibition and AMP-activated protein kinase activation. *Proc Natl Acad Sci USA* **99**: 16309–16313
- Weekes J, Ball KL, Caudwell FB, Hardie DG (1993) Specificity determinants for the AMP-activated protein kinase and its plant homologue analysed using synthetic peptides. *FEBS Lett* **334**: 335–339
- Woods A, Dickerson K, Heath R, Hong SP, Momcilovic M, Johnstone SR, Carlson M, Carling D (2005) Ca^{2+} /calmodulin-dependent protein kinase kinase-beta acts upstream of AMP-activated protein kinase in mammalian cells. *Cell Metab* **2**: 21–33
- Woods A, Johnstone SR, Dickerson K, Leiper FC, Fryer LG, Neumann D, Schlattner U, Wallimann T, Carlson M, Carling D (2003) LKB1 is the upstream kinase in the AMP-activated protein kinase cascade. *Curr Biol* **13**: 2004–2008
- Woods A, Salt I, Scott J, Hardie DG, Carling D (1996) The $\alpha 1$ and $\alpha 2$ isoforms of the AMP-activated protein kinase have similar activities in rat liver but exhibit differences in substrate specificity *in vitro*. *FEBS Lett* **397**: 347–351
- Yamauchi T, Kamon J, Minokoshi Y, Ito Y, Waki H, Uchida S, Yamashita S, Noda M, Kita S, Ueki K, Eto K, Akanuma Y, Froguel P, Foufelle F, Ferre P, Carling D, Kimura S, Nagai R, Kahn BB, Kadowaki T (2002) Adiponectin stimulates glucose utilization and fatty-acid oxidation by activating AMP-activated protein kinase. *Nat Med* **6**: 1288–1295
- Zhou G, Myers R, Li Y, Chen Y, Shen X, Fenyk-Melody J, Wu M, Ventre J, Doebber T, Fujii N, Musi N, Hirshman MF, Goodyear LJ, Moller DE (2001) Role of AMP-activated protein kinase in mechanism of metformin action. *J Clin Invest* **108**: 1167–1174